# Design Optimization of a Cost-Effective Micro Wind Turbine

D.Y.C. Leung, Y. Deng, M.K.H. Leung

*Abstract*- **The aim of this paper is to investigate the performance of a specially designed micro wind turbine for urban environment where the wind speed is usually low. Differing from the traditional wind turbine that can be connected directly to the grid, the micro wind turbine is linked to a small generator and mainly used for local applications. The advantage of the micro wind turbine is that, apart from its low cost, it can be propelled by a wind speed as low as 2 m/s. In this paper, the performance of a single micro wind turbine was evaluated through CFD analysis. The CFD simulation shows good agreement with experimental results. The validated computer model is then used for optimizing the wind turbine blade design with varying blade subtend-angle and blade number.**

*Index Terms* - **aerodynamics, angular velocity, starting torque, wind turbine blade.**

## I. INTRODUCTION

Wind energy is a clean, inexhaustible and sustainable energy source. Due to the high market demand, the development of wind energy technology has been moving very fast in many new dimensions, such as aerodynamics, structural mechanics and mechanical engineering. The main trend of wind turbine development is large-scale wind energy systems (with sizes vary from several hundreds kW to 10 MW, and rotor diameters over one hundred meters) that are often established along offshore or on vast wind sites where annual average wind speed is high.

On the other hand, a new branch of development in this field recently emerged. In regions of low wind speed and in crowded urban areas, miniature wind machines or micro wind turbines are more suitable. A small wind turbine, with a rotor diameter as small as a meter or less, can often be set up and stand alone on the roof of houses and buildings for electricity generation. This kind of wind energy converter is normally directly linked to battery rather than connected to the electric grid. As its capacity is small (usually <1kW), its prime cost is not very high and is affordable for many household applications. This micro wind turbine has received attention in recent years and a great deal of research has been conducted to optimize their performance, particularly at the low wind speed range.

D.Y.C. Leung is with the Department of Mechanical Engineering, the University of Hong Kong, Hong Kong. (Phone: 852 2858 7911, Fax: 852 2858 5415, Email: ycleung@hku.hk).

Y. Deng was with the Department of Mechanical Engineering, the University of Hong Kong, Hong Kong. He is now with Ove Arup & Partners Hong Kong Ltd..

M.K.H. Leung is with the Department of Mechanical Engineering, the University of Hong Kong, Hong Kong.

Various theoretical methods are available to calculate the aerodynamic forces on the blades of a horizontal axis wind turbine (HAWT) [1], such as the Blade Element Momentum (BEM) theory [2]-[4], Lifting Line Method (LLM) [5], Lifting Surfaces Method (LSM), N-body/particle simulation method, and asymptotic expansion method (Euler special). Among them, the BEM method is the simplest and most commonly used. This paper reports the development of a methodology for evaluating and optimizing the performance of a specially-designed low-cost micro wind turbine using a computational fluid dynamics (CFD) technique and verified the result with physical tests conducted in a wind tunnel.

## II. METHODOLOGY

### A. Wind Turbine Profile

The wind turbine under investigation is a micro fan-bladed wind turbine, as shown in Fig 1. Different from conventional two- or three-blade wind turbines, this micro wind turbine employs a fan-type blade configuration rather than an aerofoil-type, which has a functional advantage of increased power efficiency [6]. The edgewise view defines the blade thickness distribution over the blade length. Many large wind turbines utilize linear taper blades from the root to the tip for rigidity [7]. Since the blade of the micro wind turbine is not very long, it is designed to be in mono thickness along the blade length. The twist extent of the turbine blade is clearly displayed in the transaction view. Most wind turbines use twisted blades to capture a more efficient torque in different wind conditions, and the micro wind turbine in this study is no exception. The twist angle of the micro wind turbine is a critical parameter for the present computation and optimization work, and it has a strong relationship with the blade subtend-angle of the micro wind turbine. Important geometric parameters of a typical micro wind turbine under investigation are shown in the nomenclature.



Fig. 1. Micro wind turbine under studying.

The advantage of this micro fan-bladed wind turbine design is that multiple turbines can be connected together to add up the power to meet any requirements in a flexible manner. Such blade and the turbine designs can be produced by injection molding for mass production; therefore the cost of the system is only about one third of conventional wind turbine system designs.

### B. Governing Equations

Fig. 2 shows the localized forces acting on a stationary wind turbine blade. In this figure, $\Phi$, the local angle between the plane of rotation and the relative wind speed, is defined as the inflow angle. When the blade is stationary, the inflow angle $\Phi$ and the wind attack angle $\alpha$ reach their maxima and receive the maximal force F from the wind. The force F on the blade caused by the wind can be resolved into $F_{drag}$ in the axial direction and $F_{torque}$ in the tangential direction.

Fig. 3 illustrates the detailed aerodynamic analysis of the turbine blade. According to the momentum equation, the force acting on a finite element of the blade dS is:

$$dF_S = \dot{dm}(U_{rel}\sin\tau - U_{windpass}\sin\tau) \tag{1}$$

$$\dot{dm} = \rho_{air} \cdot U_{rel} \cdot dS \tag{2}$$

Combining (1) and (2),

$$dF_S = \rho_{air}(U_{rel}^2 - U_{rel} \times U_{windpass})\sin\tau \cdot dS \tag{3}$$

The axial force $dF_{S(drag)}$ and the tangential force $dF_{S(torque)}$, acting on a finite element of the blade dS, are $dF_s\sin\tau$ and $dF_s\cos\tau$, respectiverly. By summing all the axial forces $dF_{S(drag)}$ and tangential forces $dF_{S(torque)}$ of these finite elements, the total $F_{S(drag)}$ and total $F_{S(torque)}$ acting on the crossing-section of the blade can be calculated.

$$F_{S(drag)} = \int_S dF_{S(drag)} \tag{4}$$

$$F_{S(torque)} = \int_S dF_{S(torque)} \tag{5}$$

Furthermore, the axial force $F_{B(drag)}$ and the torque $T_B$ acting on a single turbine blade can be worked out by integrating all the axial forces and torques over the rotor blade length as follows:

$$F_{B(drag)} = \int_{r=R_{root}}^{r=R_{tip}} F_{S(drag)} dr \tag{6}$$

$$T_B = \int_{r=R_{root}}^{r=R_{tip}} F_{s(torque)} \, r dr \tag{7}$$

Finally, the overall drag force $F_{drag}$ and torque T acting on the whole wind turbine can be determined by multiplying the axial force $F_{B(drag)}$ and the torque $T_B$ acting on a single turbine blade with the number of blades on the wind turbine.

$$F_{drag} = N_B \cdot F_{B(drag)} \tag{8}$$

$$= N_B \cdot \int_{r=R_{root}}^{r=R_{tip}} \iint_S \rho_{air}(U_{rel}^2 - U_{rel} \cdot U_{windpass})\sin^2\tau.dSdr$$

$$T = N_B \cdot T_B \tag{9}$$

$$= N_B \cdot \int_{r=R_{root}}^{r=R_{tip}} \iint_S [\rho_{air}(U_{rel}^2 - U_{rel} \cdot U_{windpass})\sin\tau.\cos\tau.dS]rdr$$
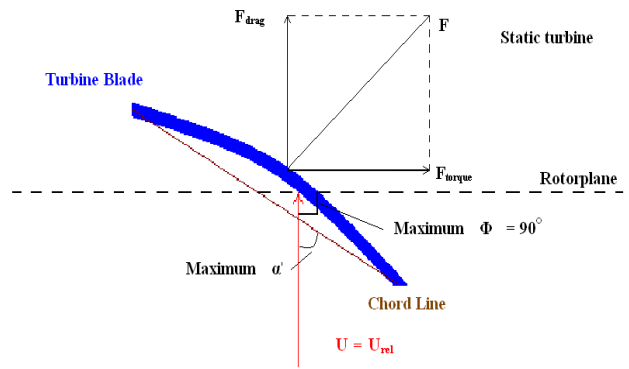


Fig. 2 Aerodynamics on a blade of the static micro wind turbine.
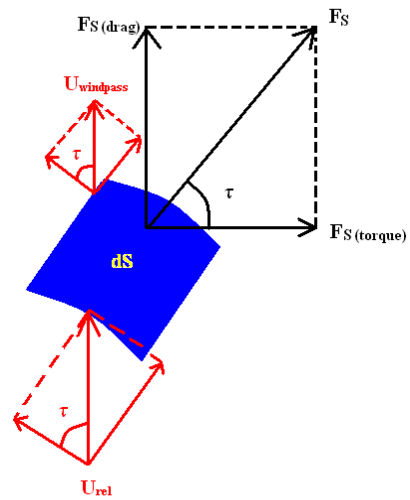


Fig. 3. Aerodynamics analysis

The wind turbine starts to rotate when the torque T is large enough to overcome the static equilibrium,. An aerodynamic analysis of the rotating wind turbine is illustrated in Fig. 4. Compared to that of the stationary one in Fig. 2, an additional vector $\omega R$ acts on the turbine blade. This is because the wind turbine is rotating with an angular velocity $\omega$ at an opposite direction. As a result, the force acting on the turbine blade is not from the wind speed U, but the relative wind speed $U_{rel}$ that is composed of the wind speed vector and the local speed vector of the blade.

### C. CFD Simulation

The CFD simulation was operated using GAMBIT 2.1 and Fluent 6.1. In the present case, the radius and the width of the micro wind turbine are 117 mm and 60 mm, respectively. A 2500mm × 2500mm × 3000mm volume was created as the computational domain with its six faces treated to be the boundaries of the domain. A uniform wind speed profile was introduced at the entrance of the domain. The micro wind turbine was set at the centre of the domain, which, together with the air inside and around it, was named as the moving-zone and was set as rotational objects in boundary conditions. The boundaries between the moving-zone and the rest of the domain are set as the interior.

Considering that the target of this research was the performance of the wind turbine, very fine grids were used to mesh the region around the wind turbine, where accurate results were demanded. Tetrahedral grid elements were introduced to discretize the domain and define the spatial resolution of the numerical solution. Triangular cells were also applied to mesh the boundary layers and inner faces. The total number of grids was about 1.5 million. The Semi-Implicit Method for Pressure-Link Equations (SIMPLE) algorithm and the standard $k - \varepsilon$ turbulence model were used to simulate the incompressible, steady-state turbulent flow.

The numerical simulations were conducted to model the performance of the micro wind turbine under different wind speeds with the aerodynamics equations stated in Section IIB.

D. Model Validation

An experiment was conducted in a wind tunnel to validate the CFD model used. A photo-sensor and a torque-meter were used to determine the angular velocity of the wind turbine and the torque acting it as shown in Fig. 4.
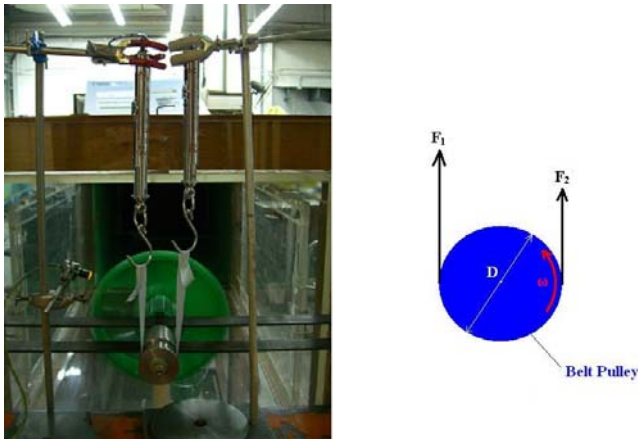


Fig. 4. Torque measurement.

E. Optimization

The optimization study was conducted by varying the blade subtend-angle of the micro wind turbine and the number of turbine blades. Table 1 shows all the simulation cases and some important parameters in the optimization work. These cases were simulated by CFD to obtain the following parameters:
- maximal angular velocity at different wind speeds;
- drag force and torque when stationary and rotating at a certain angular velocity under different wind speeds;
- mechanical energy captured by the micro wind turbine at different wind speeds.

For simplicity only a few cases will be presented here and discussed in the following sections. More information and simulation results can be found elsewhere [8].

Table 1 Computation cases and important parameters.

| Blade Subtend-Angle $\alpha$ | Blade Pitch Angle θ (tip~root) | Blade Twist Angle B | Blade No. $N_B$ | Solidity Σ (%) |
|---|---|---|---|---|
| 30° | 46.22°~67.38° | 21.16° | 12~3 | 78.4~19.6 |
| 40° | 39.07°~61.82° | 22.76° | 9~3 | 78.4~26.1 |
| 45° | 36.42°~59.49° | 23.07° | 8~3 | 78.4~29.4 |
| 60° | 31.07°~54.18° | 23.12° | 6~3 | 78.4~39.2 |
| 72° | 28.75°~51.60° | 22.85° | 5~3 | 78.4~47.0 |
| 80° | 27.91°~50.63° | 22.71° | 4~3 | 69.6~52.2 |
| 90° | 27.55°~50.19° | 22.64° | 4~3 | 78.4~58.8 |
| 100° | 27.91°~50.63° | 22.71° | 3 | 65.3 |
| 110° | 29.04°~51.94° | 22.90° | 3 | 71.8 |
| 120° | 31.07°~54.18° | 23.12° | 3 | 78.4 |

III. RESULTS

A. Modeling and Experimental Results

Fig. 5 shows the comparison of the CFD and experimental results on the maximal angular velocity of the wind turbine at different wind speeds. Without any loading, the micro wind turbine rotates freely and the angular velocity of it increased linearly with increasing wind speed in both cases. As illustrated in this figure, the experimental results match well with the modeling results.
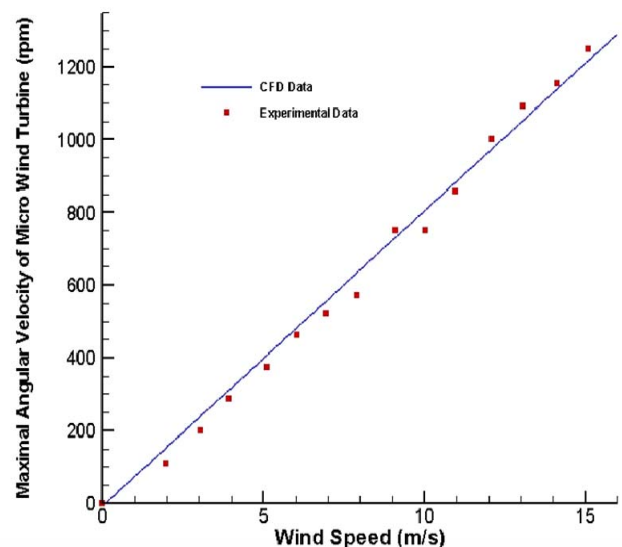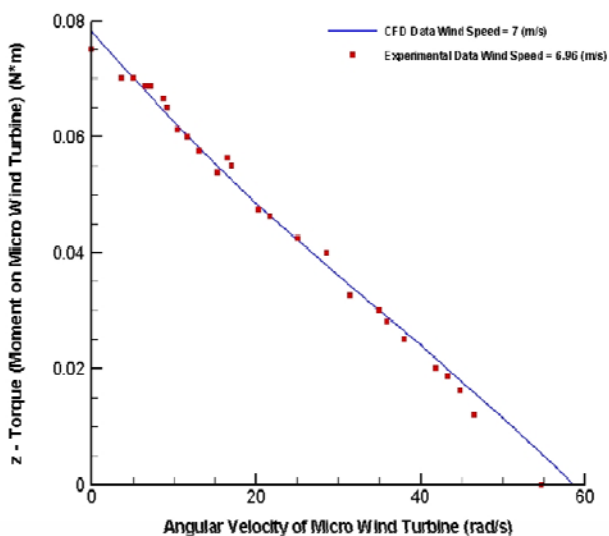


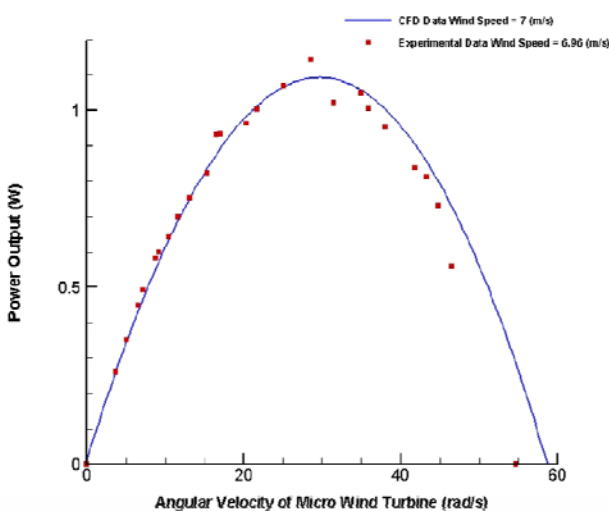Fig. 5. Maximal angular velocity Vs wind speed.

(a)



(b)



Fig. 6 Torque and power Vs angular velocity of the wind turbine at a wind speed of 7 m/s. (a) Torque; (b) Power.

Fig. 6(a) presents the comparison of the CFD and experimental results on the relationship between the torque and the angular velocity of the wind turbine at a medium wind speed (7 m/s). It can be clearly seen that the experimental data match quite well again with the numerical analysis and they both demonstrated that the torque decreased with increasing rotational velocity of the wind turbine. The relationship between the torque and maximal angular velocity is not strictly linear. Other important parameters affecting the performance are the power output and the power coefficient of the wind turbine. The power output can be worked out by multiplying the angular velocity of the turbine with the torque captured by the turbine when it was rotating at that angular velocity. Fig. 6(b) shows the relationship between the power output and the angular velocity of the wind turbine at the same wind speed. The curves indicate that the mechanical power output of the turbine increased with increasing angular velocity, reaching its maximum at the optimal angular velocity (optimal velocity), and then decreased thereafter.
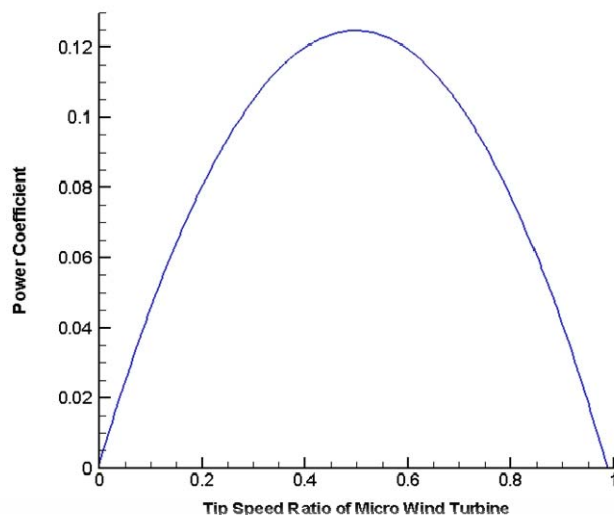


Fig 7. $C_p$- $\lambda$ characteristic of a micro wind turbine.

Fig. 7 shows the computed relationship between the power coefficient ($C_p$) and the tip speed ratio ($\lambda$) of the micro wind turbine. It is recognized that small-scale multi-bladed wind turbines normally operate at a tip speed ratio between 0 to 2 while the large-scale one with two or three blades operates at a tip speed ratio higher than 4 [9]. As indicated, the tip speed ratio of the present micro wind turbine is between 0 and 1, which meets closely with the traditional, small, multi-bladed wind turbine. Besides, the maximal power coefficient of the micro wind turbine indicates that the efficiency of the transformation from kinetic wind energy to mechanical energy is about 12%.

B. Optimization Results

To compare the performance of the micro wind turbine with different blade profiles, they were categorized into several series according to their blade subtend-angle. For each series, the blade number varied from three to a number which the blade plane of the turbine is fully-occupied. For the blades with 30-degree subtend-angle, the blade number varied from three to twelve. No significant difference in the maximal power output can be observed for the micro wind turbines with eight or more blades as shown in Fig. 8, while their maximal power outputs are much higher than those turbines with fewer blades. The optimal power coefficient of the turbines with a 30-degree blade subtend-angle is about 12.5% while the optimal tip ratio is 0.5 to 0.6 for the 8-bladed to 12-bladed profile. In addition, the maximal tip speed ratio of the micro wind turbines with different blade numbers is about the same.

To determine which of these wind turbine blade designs is optimal, the starting torque of the wind turbine needs to be considered. The larger the torque developed, the easier the wind turbine to overcome its static equilibrium. It is found from the experimental result that no obvious difference in the torque of the micro wind turbines with eight or more blades. On the other hand, a micro wind turbine rotor with fewer blades captures a smaller torque, which is not favorable for energy conversion.
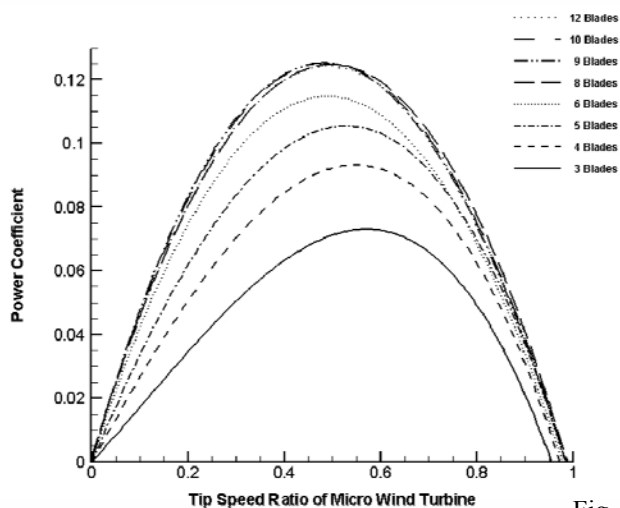
Fig.

Fig. 8 Power coefficient of the micro wind turbine with different number of blades with 30-degree blade subtend-angle.

The results of other degree subtend-angle can be found elsewhere [8]. In general, for a given blade subtend-angle, more blades yield a better performance. However, a fully-occupied rotor plane is not beneficial to both power output and starting torque of a micro wind turbine. Moreover, a blade with a subtend-angle larger than 90-degrees is not recommended design due to its poor starting performance.

## IV. DISCUSSION

Table 2 lists the solidity of the micro wind turbines and their maximal power coefficient in the optimization analysis. These data indicate that turbines with high-solidity have, in general, higher power coefficients than that of low-solidity. For the low-solidity turbines, the power coefficient increases with increasing blade subtend-angle for certain solidity. For high-solidity rotors, however, the maximal power coefficient occurs at a certain blade subtend-angle.

Table 2. Solidity of the micro wind turbines and their maximal power coefficient.

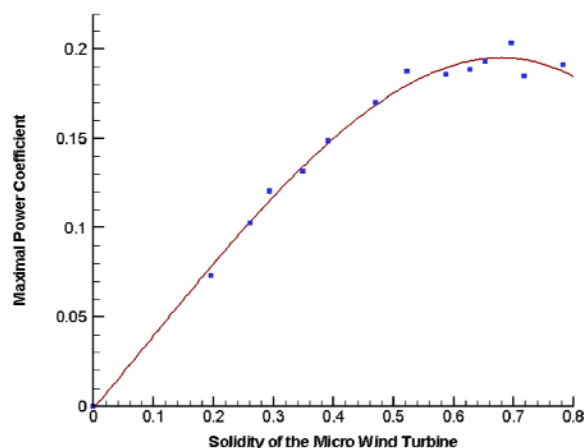| Solidity | Blade Subtend-Angle | Blade No. | Maximal Power Coefficient |
|---|---|---|---|
| 19.6% | 30° | 3 | 0.073 |
| 26.1% | 40° | 3 | 0.103 |
| 29.4% | 45° | 3 | 0.120 |
| 32.6% | 30° | 5 | 0.105 |
| 34.8% | 40° | 4 | 0.131 |
| 39.2% | 45° | 4 | 0.149 |
| 43.5% | 40° | 5 | 0.145 |
| 47.0% | 72° | 3 | 0.170 |
| 49.0% | 45° | 5 | 0.163 |
| 52.2% | 80° | 3 | 0.188 |
| 58.8% | 90° | 3 | 0.186 |
| 62.7% | 72° | 4 | 0.189 |
| 65.3% | 60° | 5 | 0.193 |
| 69.6% | 80° | 4 | 0.203 |
| 71.8% | 110° | 3 | 0.185 |
| 78.4% | 72° | 5 | 0.191 |



Fig. 9. Relationship between maximal power coefficient and solidity of wind turbine.

Fig. 9 shows the relationship between the maximal power coefficient and the solidity of the micro wind turbine. The figure illustrates that the maximal power coefficient of the turbine rises with a rising solidity in low-solidity range, and then becomes fairly stable at around 0.2, after the solidity is higher than 0.5. In other words, it is better to select a micro wind turbine profile whose solidity is higher than 0.5 to receive a higher power output.

According to the results listed in Table 2, the 4-bladed micro wind turbine with 80-degree blade subtend-angle has the highest power coefficient. However, this is not the optimal profile for the micro wind turbine due to its comparatively weak starting effect. Fig. 10 shows the torque produced by those high-efficiency wind turbine profiles under stationary condition. Among these rotors whose power coefficients are higher than 0.18, the 5-bladed rotor with 60-degree blade subtend-angle is considered to be the optimal micro wind turbine profile. Compared with that of original micro wind turbine profile (30-degree blade subtend-angle, 8-bladed), the maximal power coefficient of the 5-bladed rotor with 60-degree blade subtend-angle raises from 12.5% to 19.3%.
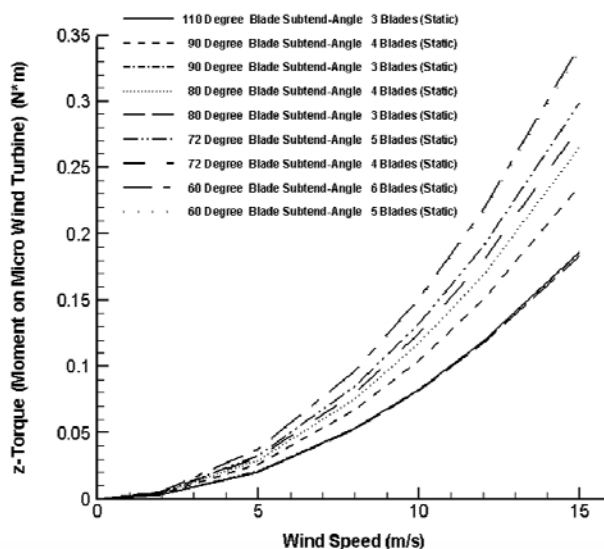


Fig. 10. Starting torque of several high-power coefficient micro wind turbines.

## V.  CONCLUSION

This study investigates the variation of the performance of micro wind turbine with different design parameters. The results showed that the performances of high-solidity wind rotors are better than those of low-solidity ones. However, for turbines with identical blade subtend-angles, one with a fully-occupied rotor may not be the best profile, since its blades block the wind acting on neighboring blades. The optimization results also show that the preferable solidity of the micro wind turbine is higher than 50%.

From the optimization analysis, it is known that rotors with larger number of blade are able to produce higher torque when they are stationary. As a result, a multi-blade approach is preferable for a micro scale wind turbine system. Considering the power coefficient and the starting effect, the 5-bladed micro wind turbine with 60-degree blade subtend-angle is the optimal turbine profile. Its maximal power coefficient is much higher than that of the preliminary turbine design (8-bladed rotor with 30-degree blade subtend-angle) and its higher power coefficient range is much wider.

## APPENDIX: NOMENCLATURE

$A_s$ : area of turbine blade projected on the cross-section
$C_p$ : power coefficient of wind turbine
$dS$ : a finite element of the turbine blade
$D$  : diameter of the belt pulley
$F$  : differential frictional force between the two readings of the spring balances
$F_{B(drag)}$ : axial force acting on a single turbine blade
$F_{drag}$ : drag force acting on the whole wind turbine
$F_{S(drag)}$ : axial force acting on the finite element $dS$
$F_{S(torque)}$ : tangential force (contributes to torque) acting on the finite element $dS$
$\dot{m}$ : mass flow rate (kg/s)
$N_B$ : number of turbine blades (present design=8)
$P_{output}$ : extracted power output of the wind turbine
$r$ : local radius
$R_{root}$ : radius of root circle of the turbine blade (present design=50mm)
$R_{tip}$ : radius of root circle of the turbine blade (present design =115mm))
$R_{turbine}$: radius of the original micro wind turbine (present design =117mm)
$T$ : torque acting on the whole turbine
$T_B$ : tangential force acting on a single turbine blade
$T_\omega$ : torque acting on the belt pulley
$U$ : upstream undisturbed wind speed
$U_{rel}$ : upstream relative wind speed
$U_{windpass}$ : downstream wind speed

$z$ : width of blade area (present design =60mm)
$\rho_{air}$ : air density
$\sigma$ : solidity of the wind turbine ($=\dfrac{N_B \times A_s}{\pi R_{turbine}^{2}}$)
(present design =52.2%)
$\omega$ : angular velocity of the wind turbine
$\lambda$ : tip speed ratio of the wind turbine
$\alpha$ : blade subtend-angle (present design =30°)
$\alpha'$ : attack angle
$\beta$ : twist angle of the turbine blade (present design =21.2°)
$\Phi$ : inflow angle
$\tau$ : the local angle between the plane of rotation and the resultant force $F_S$
$\theta$ : local angle between the chord line and the rotation plane

## REFERENCES

[1] F. Wang, L. Bai, J. Fletcher, J. Whiteford, D. Cullen, "The methodology for aerodynamic study on a small domestic wind turbine with scoop." J. Wind Eng. Ind. Aerodyn., doi: 10.1016/j. jweia. 2007. 03. 004.

[2] R. Lanzafame, M. Messina, "Fluid dynamics wind turbine design: Critical analysis, optimization and application of BEM theory." Renewable Energy 32, 2007, 2291-2305.

[3] A. Varol, C. İlkılıç, Y. Varol, "Increasing the efficiency of wind turbines." Journal of Wind Engineering and Industrial Aerodynamics 89, 2001, 809-815.

[4] M. Jureczko, M. Pawlak, A. Mężyk, "Optimization of wind turbine blades." Journal of Materials Processing Technology 167, 2005, 463-471.

[5] M.M. Duquette, K.D. Visser, "Numerical Implications of Solidity and Blade Number on Rotor Performance of Horizontal-Axis Wind Turbines." J. Solar Energy Engineering, 125, 2003, 425-432.

[6] H. Hirahara, M.Z. Hossain, M. Kawahashi,Y. Nonomura, "Testing basic performance of a very small wind turbine designed for multi-purposes." Renewable Energy 30, 2005, 1279-1297.

[7] S.M. Habali, I.A. Saleh, "Local design, testing and manufacturing of small mixed airfoil wind turbine blades of glass fiber reinforced plastics Part I: Design of the blade and root." Energy Conversion & Management 41, 2000, 249-280.

[8] Y. Deng , Design Optimization of a Micro Wind Turbine using Computational Fluid Dynamics. MPhil Thesis, The University of Hong Kong, 2008;150pp.

[9] G.L. Johnson, Wind Energy Systems, Prentice-Hall, Englewood Cliffs, New Jersey 1985.